A Convenient Method to Prepare Ag Deposited N-TiO₂ Composite Nanoparticles *via* NH₃ Plasma Treatment

Shaozheng Hu,[*] Fayun Li, and Zhiping Fan

Institute of Eco-environmental Sciences, Liaoning Shihua University, Fushun 113001, PR China
[*]*E-mail: hushaozheng001@163.com*

Ag deposited N-TiO₂ composite nanoparticles were prepared *via* NH₃ plasma treatment. X-ray diffraction, UV-vis spectroscopy, photoluminescence, and X-ray photoelectron spectroscopy were used to characterize the prepared TiO₂ samples. The plasma treatment did not change the phase composition and particle sizes of TiO₂ samples, but extended its absorption edges to the visible light region. The photocatalytic activities were tested in the degradation of an aqueous solution of a reactive dyestuff, methylene blue, under visible light. The photocatalytic activities of Ag deposited N-TiO₂ composite nanoparticles were much higher than Ag-TiO₂, N-TiO₂, and P25. A possible mechanism for the photocatalysis was proposed.

Key Words : NH₃ plasma, Ag, TiO₂, Photocatalysis, Visible light

Introduction

TiO₂ is the most frequently used photocatalyst material and has been used in transforming toxic organic molecules to H₂O, CO₂ and other harmless molecules.[1-3] This property has been applied in removing bacteria and harmful organic materials from water and air, as well as in self-cleaning or self-sterilizing surfaces for places such as medical centers. However, because of the wide band gap of TiO₂ (*ca.* 3.2 eV for anatase), its practical application is inhibited for the low photon utilization efficiency and need of an UV excitation which accounts for only small fraction of the solar light (3-5%). Therefore, it is highly desirable to develop TiO₂-based photocatalysts with enhanced activities under visible light.

In 2001, Asahi *et al.*[3] prepared nitrogen doped TiO₂ films by sputtering TiO₂ in a N₂/Ar gas mixture, and concluded that the doped N atoms narrowed the band gap of TiO₂ by mixing N 2p and O 2p states, therefore demonstrating the activity for the decomposition of acetone and methylene blue. Since then, N-doping has become a hot topic and been widely investigated. Heating TiO₂ powders in N₂ and/or NH₃ at elevated temperatures is the conventional method to prepare nitrogen-doped TiO₂.[3] Besides the energy waste, the treatment at such high temperature usually results in the low surface area due to the undesirable sintering of nano-crystallites. Therefore, new strategies for preparing nitrogen-doped TiO₂, such as sputtering, sol-gel, ion implantation, pulsed laser deposition, hydrothermal synthesis, and nitrogen-plasma treatment have been proposed recently.[4-9]

Besides, modification with metal, especially noble metal, has been proved to be a effective method to improve visible light activity. Tian *et al.*[10] prepared the gold-loaded TiO₂ (Au/N-TiO₂) nanoparticles by a simple wet-chemical method. The visible light activity of modified catalysts in 2,4-di-chlorophenol (2,4-DCP) degradation were much higher than that of pure TiO₂. Kim *et al.* prepared Pt ion-doped TiO₂,

and reported its improved visible light activity for the photo-degradation of chlorinated organic compounds.[11] Ashkarran *et al.*[12] reported that the antibacterial activity of the prepared Ag/TiO₂ nanoparticles improved obviously compared with that of pure TiO₂. Among the noble metals, Ag is the one most cheap. In the past decade, the research for preparation of Ag/TiO₂ nanocomposites has mainly been focused on the control of size, shape, and dispersion of the metal particles. Several approaches have succeeded in providing desired characteristics, such as chemical, electrochemical, sono-chemical or photocatalytic methods.[13-16] In those processes, the reduction of silver salts is normally achieved by intro-duction of a variety of reductants, organic stabilizers or micells,[17,18] which always bring difficulties in separating additives from the system, and thus the catalytic activity is depressed to a considerable extent.

In this work, Ag deposited N-TiO₂ composite nanoparticles were prepared conveniently *via* NH₃ plasma treatment. Ag was reduced by the active nitrogen species which produced by the NH₃ plasma. The photocatalytic activities were tested in the degradation of an aqueous solution of a reactive dyestuff, methylene blue, under visible light. A possible mechanism for the photocatalysis was proposed.

Experimental

Preparation and Characterization. The sample N-TiO₂ was prepared according to the previous literature.[19] The doping of TiO₂ was conducted in a dielectric barrier dis-charge (DBD) reactor, consisting of a quartz tube and two electrodes. The high-voltage electrode was a stainless-steel rod (2.5 mm), which was installed in the axis of the quartz tube and connected to a high voltage supply. The grounding electrode was an aluminum foil which was wrapped around the quartz tube. For each run, 0.4 g commercial TiO₂ powder (P25) was charged into the quartz tube. At a constant NH₃

flow (40 mL min^{-1}), a high voltage of 9-11 kV was supplied by a plasma generator at an overall power input of 50 V × 0.4 A. The discharge frequency was fixed at 10 kHz, and the discharge was kept for 15 min. After discharge, the reactor was cooled down to room temperature. The obtained TiO_2 sample was denoted as N-TiO_2.

For Ag deposited N-TiO_2 composite nanoparticles, a mount of $AgNO_3$ (molar ratio Ag/Ti = 0.01, 0.02, and 0.03) was dissolved in 20 mL water. P25 was added into above solution under stirring. The formed suspension was stirred for 30 min. The formed suspension was dried at 100 °C for 2 h to obtain the Ag-TiO_2 precursor. For each run, 0.4 g Ag-TiO_2 precursor was charged into the quartz tube following the same procedure above. The obtained Ag deposited N-TiO_2 composite nanoparticles were denoted as AN1-TiO_2, AN2-TiO_2, and AN3-TiO_2. When H_2 was used to replace NH_3 following the same procedure as in the synthesis of AN2-TiO_2, the product is denoted as Ag-TiO_2.

XRD patterns of the prepared TiO_2 samples were recorded on a Rigaku D/max-2400 instrument using Cu-Kα radiation (λ = 1.54 Å). UV-Vis spectroscopy measurement was carried out on a Jasco V-550 spectrophotometer, using $BaSO_4$ as the reference sample. Photoluminescence (PL) spectra were measured at room temperature with a fluorospectrophotometer (FP-6300) using an Xe lamp as excitation source. XPS measurements were conducted on a Thermo Escalab 250 XPS system with Al Kα radiation as the exciting source. The binding energies were calibrated by referencing the C 1s peak (284.6 eV) to reduce the sample charge effect. Photoelectrochemical experiments were carried out in a glass cell using a three-electrode system controlled by a VoltaLab 40 potentiostat (PGZ 301, Radiometer analytical). The electrolyte used in this study was 0.5 M Na_2SO_4. A Pt coil was used as the counter electrode and was flame annealed before each experiment. A saturated Ag/AgCl electrode was used the reference electrode. The synthesized TiO_2 materials were used as the working electrode. For visible light irradiance, the light from the source was passed through an optical filter, which cut off wavelengths below 420 nm. The intensity of the resulting visible light was 0.02 mW/cm^2.

Photocatalytic Reaction. Methylene blue (MB) was selected as model compound to evaluate the photocatalytic performance of the prepared TiO_2 particles in an aqueous solution under visible light irradiation. 0.1 g of TiO_2 powders were dispersed in 100 mL MB solution (50 ppm) in an ultrasound generator for 10 min. The suspension was transferred into a 250 mL beaker and stirred for 30 min in darkness to achieve the adsorption equilibrium. For photoreaction under visible light irradiation, the suspension was exposed to a 110-W high-pressure sodium lamp with main emission in the range of 400-800 nm, and bubbled with air (130 mL/min). The light from the source was passed through an optical filter, which cut off wavelengths below 420 nm. The light intensity is 130 mWcm^{-2}. All runs were conducted at ambient pressure and 30 °C. At given time intervals, 4 mL suspension was taken and immediately centrifuged to separate the liquid samples from the solid catalyst. The concen-

trations of MB before and after reaction were measured by means of a UV-Vis spectrophotometer at a wavelength of 665 nm. It is the linear relationship between absorbance and concentration of liquid sample in the experimental concentration range. Therefore, the percentage of degradation *D%* was determined as follows:

$$D\% = \frac{A_0 - A}{A_0} \times 100\% \qquad (1)$$

Where A_0 and A are the absorbances of the liquid sample before and after degradation, respectively.

Results and Discussion

Figure 1 shows the XRD patterns of the prepared TiO_2 particles and a commercial TiO_2 powder (P25). It is indicated that each sample was a mixture of anatase and rutile phases. The phase contents of the samples were estimated from their XRD patterns by the following equation:[20]

$$x_A = \frac{1}{1 + 1.26 \times \dfrac{I_R}{I_A}} \qquad (2)$$

where x_A is the fraction of anatase phase, I_R and I_A are the intensities of the anatase (101) and rutile (110) diffraction peaks, respectively. The contents of anatase phase in P25, Ag-TiO_2, N-TiO_2, and AN-TiO_2 were 0.755, 0.757, 0.761, and 0.753. Besides, the particle sizes of P25, N-TiO_2, and AN-TiO_2 which calculated by their XRD patterns according to the Debye-Scherrer equation were 25.1, 26.3, 26.2, and 26.4 nm.[21] These results indicate that there were no obvious changes in phase composition and particle sizes after plasma treatment. It is noteworthy that no other crystalline phase containing Ag was observed. This result can likely be explained that the very fine dispersion of metallic Ag or oxide was formed on the titania which is below the detection limit of this technique.

UV-Vis spectra of P25 and prepared TiO_2 composites are shown in Figure 2. P25 showed no absorption in visible light region. For Ag-TiO_2, an additional absorption band around
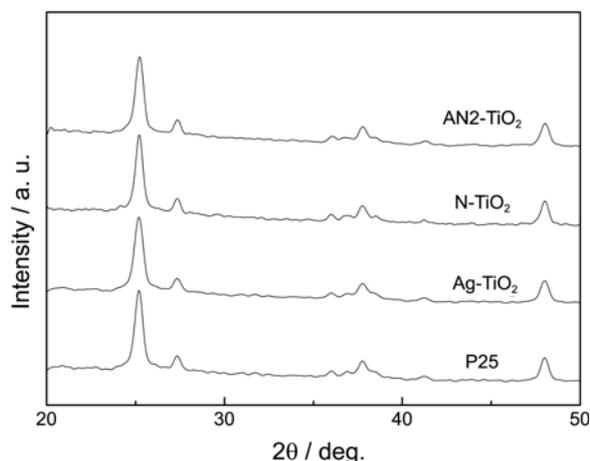

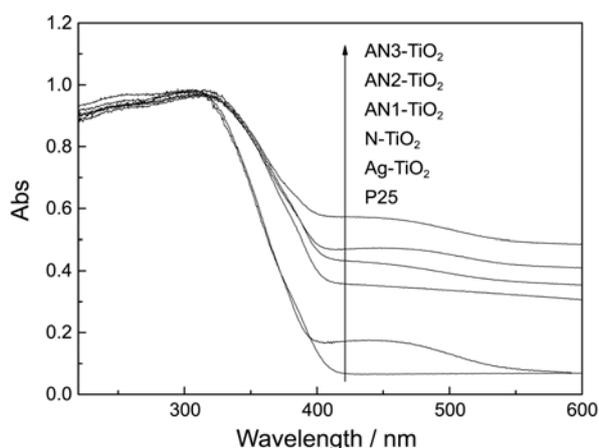**Figure 1.** XRD patterns of P25 and prepared TiO_2 particles.

Figure 2. UV-vis spectra of P25 and prepared TiO₂ composites.

Figure 3. XP spectra of P25, N-TiO₂, and AN2-TiO₂ in the region of Ti 2p (a) and N 1s (b).

450 nm was observed. This is caused by the surface plasmon absorption of metallic Ag.[23] The distinct shifts of the absorption edges into visible light region were observed for all the NH_3 plasma treated TiO_2 materials. The band gap energies of TiO_2 samples were calculated according to the method of Oregan and Gratzel.[22] It is known that the band gap of P25 and Ag-TiO₂ are 3.2 eV. For NH_3 plasma treated TiO_2 materials, N-TiO₂, AN1-TiO₂, AN2-TiO₂, and AN3-TiO₂, this value decreased to 2.82, 2.8, 2.8, and 2.75 eV, respectively. These absorption edges shifts are due to the electronic transition from the isolated N 2p level, which is formed by incorporation of nitrogen atoms into the TiO_2 lattice, to the conduction band.[24] Besides, the additional absorption band around 450 nm in Ag deposited N-TiO₂ indicated that the metallic Ag existed. According to our previous investigation,[19] this is probably due to that NH_3 plasma consists of not only various active nitrogen species but excited hydrogen, leading to Ag reduced. Therefore, it is reasonable that Ag was existed as not oxide but metallic state on the TiO_2 surface.

XPS is an effective surface test technique for characterizing elemental composition and chemical states. The binding energy of the element is influenced by its electron density. A decrease in binding energy implies an increase of the electron density. Figure 3 shows the XP spectra of P25, N-TiO₂, and AN2-TiO₂ in the region of Ti 2p (A) and N 1s (B). Compared with the spectra of P25, slight shifts to lower binding energies were observed for N-TiO₂ in the Ti 2p region (458.4 eV). This is probably attributed to the change of chemical environment after N doping.[25] The electrons of the lone electron pair of N atoms may be partially transferred from N to Ti, due to the higher electronegativity of oxygen, leading to increased electron densities on Ti atoms.

XP spectra of N-TiO₂, and AN2-TiO₂ in the region of N 1s are shown in Figure 3(b). Up to now, the assignment of the XPS peak of N1s is still under debate. Since the preparation methods and conditions considerably affect nitrogen XPS spectral features, the peak positions may be different from different literatures. In addition, the different nitrogen source may also influence the characteristics of the nitrogen state.
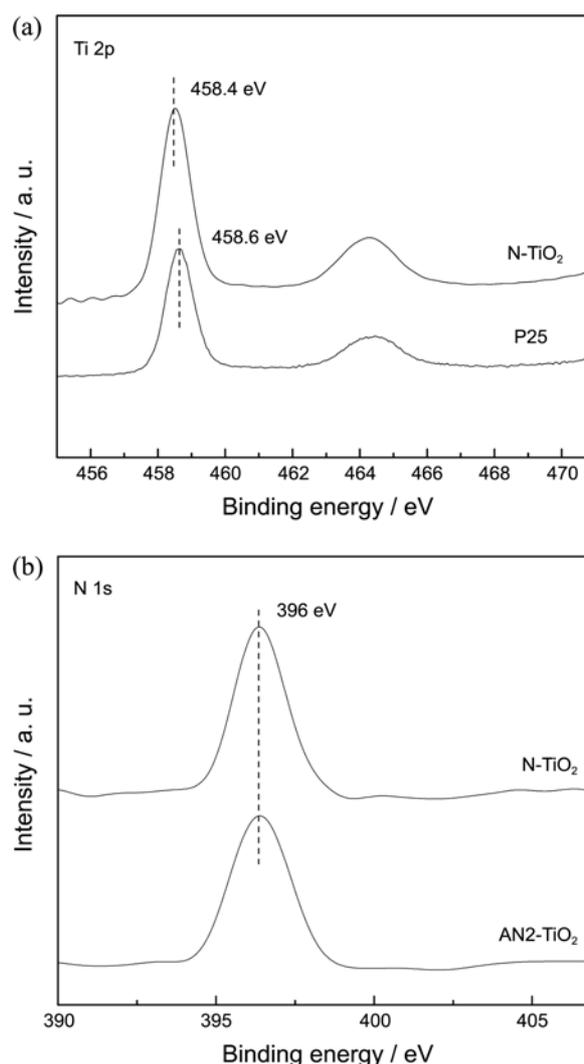
Cong *et al.*[26] reported that the peak in the range of 397-401 eV was the N1s peak when using the wet chemical method, whereas other methods should exhibit the N1s peak around 396 eV. Besides, according to the previous literatures about prepration of N doped TiO_2 using N_2 plasma treatment,[27] the peaks around 396 eV are attributed to substitution of crystal-lattice oxygen of TiO_2 to form Ti-N bond. Therefore, it is indicated that N atoms were doped into TiO_2 crystal-lattice successfully by NH_3 plsama treatment.

XP spectra of AN2-TiO₂ (a) and Ag-TiO₂ (b) in the region of Ag 3d before and after NH_3 plasma treatment are shown in Figure 4. Before plasma treatment, the peaks around 367.3 and 373.3 eV are attributed to the AgO,[28] indicating Ag existed as oxide before plasma treatment. After plasma treatment, the spectrum confined to the Ag presents the binding energies of the Ag $3d_{5/2}$ and Ag $3d_{3/2}$ peaks corresponding to 368.1 and 374.1 eV, respectively. Therefore, the Ag clusters existed in metallic form.[29] Therefore, it is indicated that AgO were reduced to metallic Ag successfully by NH_3 or H_2 plsama treatment.
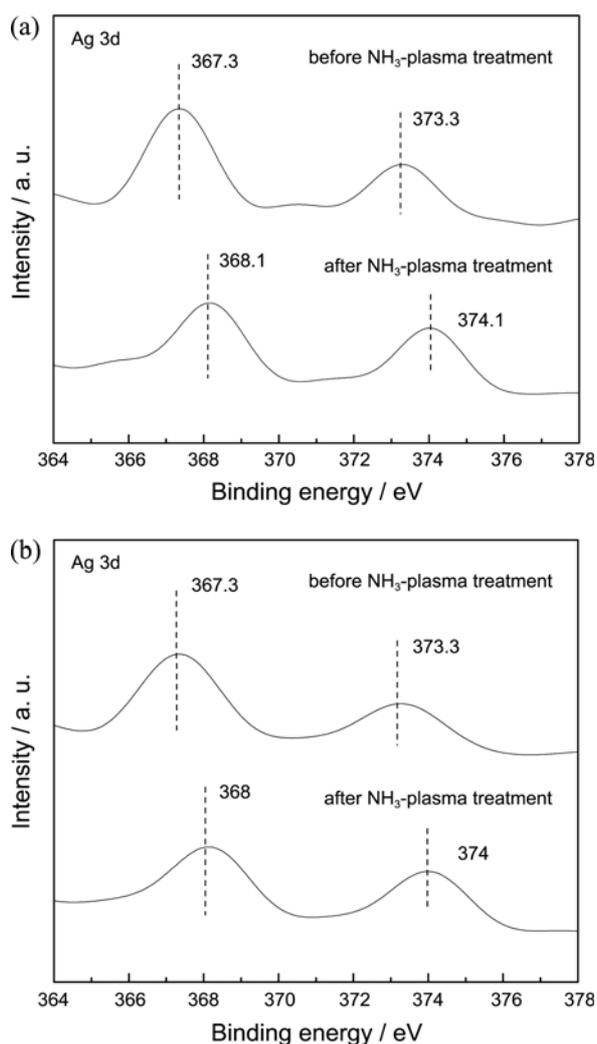
Figure 4. XP spectra of AN2-TiO$_2$ (a) and Ag-TiO$_2$ (b) in the region of Ag 3d before and after plasma treatment.

Figure 5. Variation of photocurrent density *vs* applied electrode potential for the P25 and prepared TiO$_2$ composites in 0.5 M Na$_2$SO$_4$ electrolyte under visible light irradiation.

Figure 6. Photoluminescence emission spectra of plasma treated TiO$_2$ particles.

Figure 5 shows a comparison of the photocurrent density *vs* applied potential curves for the P25 and P25 and prepared TiO$_2$ composites under visible light irradiation. As expected, the photocurrent of P25 and Ag-TiO$_2$ were very low and did not change with increased applied potential. After N doping, the photocurrent of N-TiO$_2$ increased with increasing the applied potential. Interestingly, the synthesized AN2-TiO$_2$ showed much higher photocurrent than other samples, demonstrating that AN2-TiO$_2$ can more effectively harvest visible light. This is probably due to the synergistic effect of Ag and N. This is consistent with the UV-vis results shown in Figure 2.

PL emission spectrum, which is closely related to surface states and stoichiometric chemistry, is used to determine the efficiency of trapping, migration, and transfer of a charge carrier, and to understand the fate of electron-hole pairs in semiconductors. Figure 6 shows the PL spectra of plasma treated TiO$_2$ using excitation at 300 nm. All the samples showed two emission peaks at 426 and 450 nm. The emission at 426 nm with band g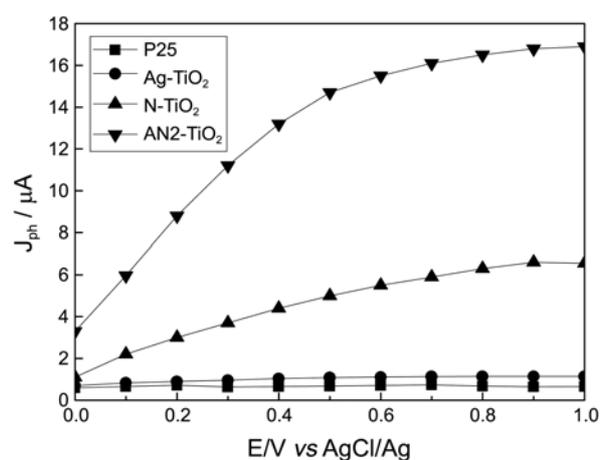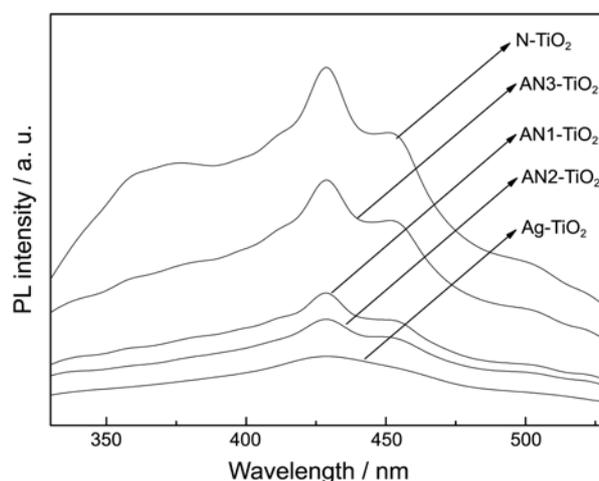ap energy of 2.9 eV can be attributed to the free exciton, O^{2-} → Ti^{4+} charge-transfer transition. The emission at 450 nm corresponding to 2.75 eV, which is approximately equal to the band-gap of plasma treated TiO$_2$ materials, can be due to the transition from isolated N 2p level to the conduction band of TiO$_2$. Besides, it is also observed that the intensity of the luminescence peaks reduces for Ag deposited N-TiO$_2$ composite nanoparticles. As the PL emission is the result of the recombination of excited electrons and holes, the lower PL intensity indicates the decrease in recombination rate, thus higher photocatalytic activity.[30] Therefore, this can be ascribed to the decreased recombination of charge-carriers, which are trapped in the Ag 3d energy level below the conduction band in the Ag deposited N-TiO$_2$ composite nanoparticles.[31] The PL intensity of Ag deposited N-TiO$_2$ composite nanoparticles decreased in the order: AN3-TiO$_2$ > AN1-TiO$_2$ > AN2-TiO$_2$. This indicated that excess amount of Ag in AN3-TiO$_2$ sample will act as the recombination center of electrons and holes, leading to the low quantum efficiency.

Figure 7 presents the photocatalytic performances of P25 and plasma treated TiO$_2$ composite nanoparticles in the
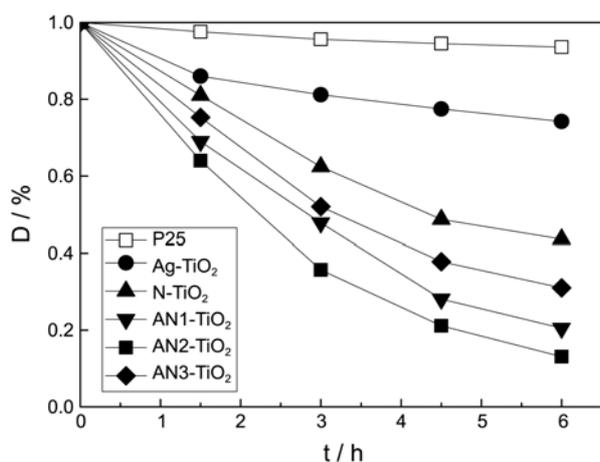
Figure 7. Photocatalytic performances of P25 and plasma treated TiO₂ composite nanoparticles in the degradation MB under visible light irradiation.

degradation MB under visible light irradiation. It is shown that P25 exhibited poor activity under visible light. After Ag depositing, the activity of Ag-TiO₂ improved slightly. However, the photocatalytic activity of N-TiO₂ improved obviously compared with P25 and Ag-TiO₂. Since no obvious change were observed in phase compositions and particle sizes between P25 and N-TiO₂, the enhanced photocatalytic activity must result from the doping of nitrogen in TiO₂, which gave rise to the narrowed band gap and thus to the enhanced absorption in the visible region. Moreover, after Ag deposition, the photocatalytic activities further improved for AN1-TiO₂, AN2-TiO₂, and AN3-TiO₂. This is attributed to that the photogenerated electrons were trapped by the deposited Ag, leading to the decreased recombination rate (Fig. 6). Besides, it is shown in Figure 7 that the activity improved firstly then deceased obviously when increased the Ag concentration. This is probably due to the following two reasons. First one, excess amount of Ag in AN3-TiO₂ sample will act as the recombination center of electrons and holes, leading to the low quantum efficiency, which has been proved by the PL result. Second one, the excess amount of Ag deposited on TiO₂ surface may influence the penetration of visible light, thus decreased the quantum efficency, leading to the decreased activity.

Figure 8. XP spectra of Ag-TiO₂ (a) and AN2-TiO₂ (b) in the region of Ag 3d before and after MB degradation reaction. For Ag-TiO₂, it is shown that the binding energy of Ag 3d shifted to 367.4 and 373.4 eV after MB degradation reaction. This indicated that the metallic Ag was oxided to AgO after reaction. However, for the spectra of AN2-TiO₂, the binding energy of Ag 3d was not changed before and after MB degradation reaction (368.1 and 374.1 eV), indicating the metallic Ag was not oxided. This further proved that the synergistic effect of Ag and N existed which restrained the formation of AgO.

Scheme 1 illustrates the mechanism of the photocatalytic degradation over Ag deposited N-TiO₂ composite nanoparticles under visible light irradiation. Under visible light
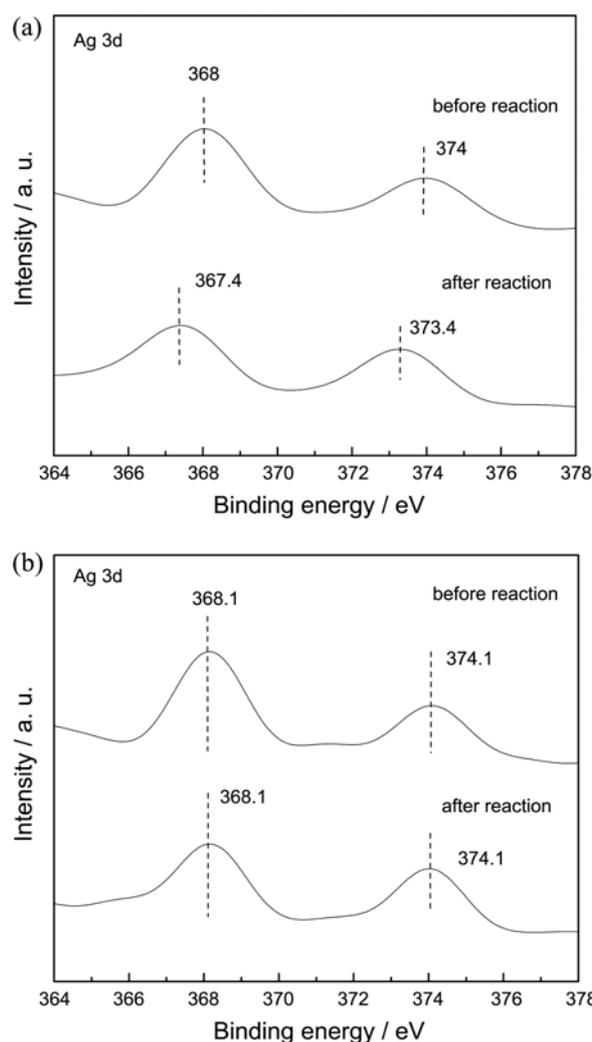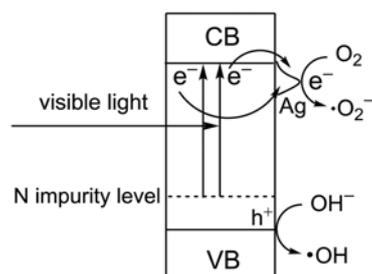

Figure 8. XP spectra of Ag-TiO₂ (a) and AN2-TiO₂ (b) in the region of Ag 3d before and after MB degradation reaction.

Scheme 1. Mechanism of the photocatalytic degradation over Ag deposited N-TiO₂ composite nanoparticles under visible light irradiation.

irradiation, electrons are excited from the N impurity energy level to the conduction band of TiO₂. Subsequently, they are captured by deposited Ag and then transferred to the adsorbed O₂ on the surface of TiO₂ rapidly to form superoxide anion radicals (•O₂⁻), which can further initiate the degradation reaction. Simultaneously, the photogenerated holes which left in the valence band react with OH⁻ to form highly active oxygen species •OH. The generated •OH and

•O_2^- species are responsible for the degradation of MB. Therefore, the presence of Ag can restrain the recombination of photo-induced electrons and holes, resulting in the enhancement of photocatalytic activity. However, excess amount of Ag not only influences the penetration of visible light but also acts as the recombination center of electrons and holes, leading to the decrease of photocatalytic activity.

Conclusions

Ag deposited N-TiO$_2$ composite nanoparticles were prepared *via* NH$_3$ plasma treatment. The plasma treatment did not change the phase composition and particle sizes of the pristine TiO$_2$, but extended its absorption edges to the visible light region. UV-vis and XPS results showed that AgO were reduced to metallic Ag by NH$_3$ plsama treatment. The metallic Ag which deposited on TiO$_2$ surface trapped photogenerated electrons, leading to the reduced recombination of charge-carriers. Photoelectrochemical experiments and XPS results proved the synergistic effect of Ag and N existed in Ag deposited N-TiO$_2$ composite nanoparticles. The photocatalytic activity of Ag deposited N-TiO$_2$ composite nanoparticles were much higher than that of P25 and N-TiO$_2$. This is due to not only the narrowed band gap energy which caused by the N doping, but also the decreased recombination of charge-carriers by Ag depositing.

References

1. Fujishima, A.; Honda, K. *Nature* **1972**, *238*, 37.
2. Hoffmann, M. R.; Martin, S. T.; Choi, W.; Bahnemann, D. W. *Chem. Rev.* **1995**, *95*, 69.
3. Asahi, R.; Morikawa, T.; Ohwaki, T.; Aoki, A.; Taga, Y. *Science* **2001**, *293*, 269.
4. Lindgren, T.; Mwabora, J. M.; Avendano, E.; Jonsson, J.; Hoel, A.; Granqvist, C. G.; Lindquist, S. E. *J. Phys. Chem. B* **2003**, *107*, 5709.
5. Qiao, M.; Wu, S. S.; Chen, Q.; Shen, J. *Mater. Lett.* **2010**, *12*, 1398.
6. Shen, H.; Mi, L.; Xu, P.; Shen, W. D.; Wang, P. N. *Appl. Surf. Sci.* **2007**, *17*, 7024.
7. Zhao, L.; Jiang, Q.; Lian, J. S. *Appl. Surf. Sci.* **2008**, *15*, 4620.
8. Hu, S. Z.; Wang, A. J.; Li, X.; Löwe, H. *J. Phys. Chem. Solid* **2010**, *71*, 156.
9. Hu, S. Z.; Li, F. Y.; Fan, Z. P. *Appl. Surf. Sci.* **2011**, *258*, 1249.
10. Tian, B. Z.; Li, C. Z.; Gu, F.; Jiang, H. B. *Catal. Commun.* **2009**, *10*, 925.
11. Kim, S.; Hwang, S. J.; Choi, W. *J. Phys. Chem. B* **2005**, *109*, 24260.
12. Ashkarran, A. A.; Aghigh, S. M.; kavianipour, M.; Farahani, N. J. *Curr. Appl. Phys.* **2011**, *11*, 1048.
13. Li, X.; Zhang, J.; Xu, W.; Jia, H.; Wang, X.; Yang, B.; Zhao, B.; Li, B.; Ozaki, Y. *Langmuir* **2003**, *19*, 4285.
14. Yin, B.; Ma, H.; Wang, S.; Chen, S. *J. Phys. Chem. B* **2003**, *107*, 8898.
15. Pol, V. G.; Srivastava, D. N.; Palchik, O.; Palchik, V.; Slifkin, M. A.; Weiss, A. M.; Gedanken, A. *Langmuir* **2002**, *8*, 3352.
16. Zhang, L. Z.; Yu, J. C. *Catal. Commun.* **2005**, *6*, 684.
17. Cozzoli, P. D.; Comparelli, R.; Fanizza, E.; Curri, M. L.; Agostiano, A.; Laub, D. *J. Am. Chem. Soc.* **2004**, *126*, 3868.
18. Wang, Z.; Chen, M.; Wu, L. *Chem. Mater.* **2008**, *20*, 3251.
19. Hu, S. Z.; Li, F. Y.; Fan, Z. P. *J. Hazard. Mater.* **2011**, *196*, 248.
20. Spurr, R. A.; Myers, H. *Anal. Chem.* **1957**, *29*, 760.
21. Lin, J.; Lin, Y.; Liu, P.; Meziani, M. J.; Allard, L. F.; Sun, Y. P. *J. Am. Chem. Soc.* **2002**, *124*, 11514.
22. Oregan, B.; Gratzel, M. *Nature* **1991**, *353*, 737.
23. Ren, L. L.; Zeng, Y. P.; Jiang, D. L. *Catal. Commun.* **2009**, *10*, 645.
24. Ozaki, H.; Fujimoto, N.; Iwamoto, S.; Inoue, M. *Appl. Catal. B* **2007**, *70*, 431.
25. Li, H. X.; Li, J. X.; Huo, Y. N. *J. Phys. Chem. B* **2006**, *110*, 1559.
26. Cong, Y.; Zhang, J. L.; Chen, F.; Anpo, M.; He, D. N. *J. Phys. Chem. C* **2007**, *111*, 10618.
27. Yamada, K.; Yamane, H.; Matsushima, S.; Nakamura, H.; Ohira, K.; Kouya, M.; Kumada, K. *Thin Solid Films* **2008**, *516*, 7482.
28. Bao, X.; Muhler, M.; Schedel-Niedrig, Th.; Schlögl, R. *Phys. Rev. B* **1996**, *54*, 2249.
29. Zhang, H. M.; Liang, C. H.; Liu, J.; Tian, Z. F.; Wang, G. H.; Cai, W. P. *Langmuir* **2012**, *28*, 3938.
30. Ozaki, H.; Iwamoto, S.; Inoue, M. *J. Phys. Chem. C* **2007**, *111*, 17061.
31. Nagaveni, K.; Hegde, M. S.; Madras, G. *J. Phys. Chem. B* **2004**, *108*, 20204.